



Density control on self-assembling of Ge islands using carbon-alloyed strained SiGe layers

A. Bernardi, M. I. Alonso, A. R. Goñi, J. O. Ossó, and M. Garriga

Citation: [Applied Physics Letters](#) **89**, 101921 (2006); doi: 10.1063/1.2349317

View online: <http://dx.doi.org/10.1063/1.2349317>

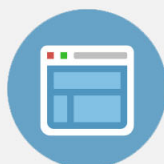
View Table of Contents: <http://scitation.aip.org/content/aip/journal/apl/89/10?ver=pdfcov>

Published by the [AIP Publishing](#)



Re-register for Table of Content Alerts

Create a profile.



Sign up today!



Density control on self-assembling of Ge islands using carbon-alloyed strained SiGe layers

A. Bernardi,^{a)} M. I. Alonso, A. R. Goñi, J. O. Ossó, and M. Garriga
Institut de Ciència de Materials de Barcelona-CSIC, Esfera UAB, 08193 Bellaterra, Spain

(Received 26 May 2006; accepted 18 July 2006; published online 8 September 2006)

The authors show that by deposition of 0.1 ML of carbon prior to the self-assembled growth of Ge quantum dots on a strained Si_{1-x}Ge_x buffer layer a striking decrease in dot density by two orders of magnitude from about 10¹¹ to 10⁹ cm⁻² occurs when the Ge content of the buffer layer increases from 0% to 64%. Their results give experimental evidence for a kinetically limited growth mechanism in which Ge adatom mobility is determined by chemical interactions among C, Si, and Ge. Thus, by adjusting the Ge content of the SiGe buffer layer onto which a carbon submonolayer is deposited they are able to fine tune the density of the carbon-induced Ge quantum dots. © 2006 American Institute of Physics. [DOI: 10.1063/1.2349317]

Size, density, shape uniformity, and ordering^{1,2} of quantum dots (QDs) are crucial parameters when self-assembling is considered for applications in optoelectronic devices. In recent years, different smart strategies have been proposed to address the problem of dot engineering.³ Increase of dot density at very low substrate temperatures and/or high deposition rates is a well established technique but in most cases it is not of practical interest for applications due to the degradation of crystalline quality. Perfect position control keeping high quality of dot ensembles can be achieved by means of artificially nanopatterned substrates.⁴ This approach is, however, less suitable for potential high-surface and low cost applications. An alternative are spontaneous bottom up approaches such as the use of template layers to guide the selective nucleation of dots, which has demonstrated to be a good method to control the positioning of dots by inducing self-ordering processes during growth. A strain-driven instability^{5,6} in SiGe/Si(001) pseudomorphic layers leads to the formation of periodic surface undulations (ripples) acting as a natural template pattern^{7,8} that can be controlled by thickness, composition, and selection of vicinal Si(001) surfaces.⁹ Other routes include Ge deposition on relaxed SiGe/Si buffer layers^{10,11} and deposition on buried dislocation networks.¹² Another relevant bottom up strategy towards efficient dot engineering involves surface modification through deposition of sub monolayer amounts of impurities¹³ that can reduce the diffusion length (i.e., enhancing dot density) and alter the energetics of nucleation. This approach has recently gathered renewed interest, having as examples the cases of surfactant mediated growth in the presence of Sb (Ref. 9) or surface alloying with carbon.^{14,15}

In this Letter we present a different route for manipulating Ge island self-assembling based on the combination of epitaxial growth on strained SiGe buffer layers and carbon predeposition. Inspired by our recent results on the influence of Si interdiffusion and the Ge–C repulsive interaction on the resulting Ge dot topography¹⁵ we make use of the effect that a submonolayer deposition of C has on the Ge adatom diffusion. Our results point to a reduction by two orders of magnitude of dot density with increasing Ge content in the buffer layer. This experimental evidence is in frank contrast

with currently accepted models for island nucleation in the absence of carbon. We therefore propose a growth scenario in which the Ge–C chemical interaction plays a determinant role.

The growth sequence of the uncapped Ge QDs prepared by solid-source molecular beam epitaxy on Si(001) substrates is as follows. After desorbing the thin oxide of the Si wafer at 900 °C and depositing a 50 nm thick Si buffer layer, the substrate temperature was set to 400 °C to deposit a thin strained Si_{1-x}Ge_x buffer layer with Ge composition x ranging from 0% to ~60%. For all the samples the SiGe buffer layer thickness (see Table I) remained below the limit of metastability,^{16,17} preventing three-dimensional nucleation of SiGe quantum dots, as confirmed by *in situ* reflection high-energy electron diffraction monitoring. The temperature was then raised and maintained at 500 °C during the deposition of 0.1 ML of carbon by a sublimation filament and the subsequent evaporation of ~6 Å of Ge at a fixed growth rate of ~0.04 Å/s, leading to self-assembling of quantum dots.

In Fig. 1 we present the topographic images obtained with an atomic force microscope (AFM) resulting from the three-step deposition process (SiGe buffer+carbon+Ge) with different compositions x of the buffer layer, maintaining the remaining growth parameters fixed. At low Ge content in the buffer layer, carbon induces the nucleation of a high density of small dome-shaped dots with monomodal size distribution [see Fig. 1(a)], similar to what was previously observed in the case of C predeposition directly on Si(001).¹³ By increasing the Ge composition of the buffer layer we observe a significant decrease of island density [see Figs.

TABLE I. Composition values and layer thicknesses obtained by optical characterization of the Si_{1-x}Ge_x buffer layers using spectral ellipsometry and Raman scattering.

Ellipsometry		Raman	
Thickness (nm)	Composition x	ω_{SiGe} (cm ⁻¹)	Composition x
5±1	0.08±0.02	404.3±0.5	0.08±0.01
8±1	0.20±0.02	410.3±0.5	0.25±0.05
7±1	0.44±0.01	418.3±0.2	0.43±0.08
6±1	0.64±0.01	421.3±0.1	0.63±0.01

^{a)}Electronic mail: abernardi@icmab.es

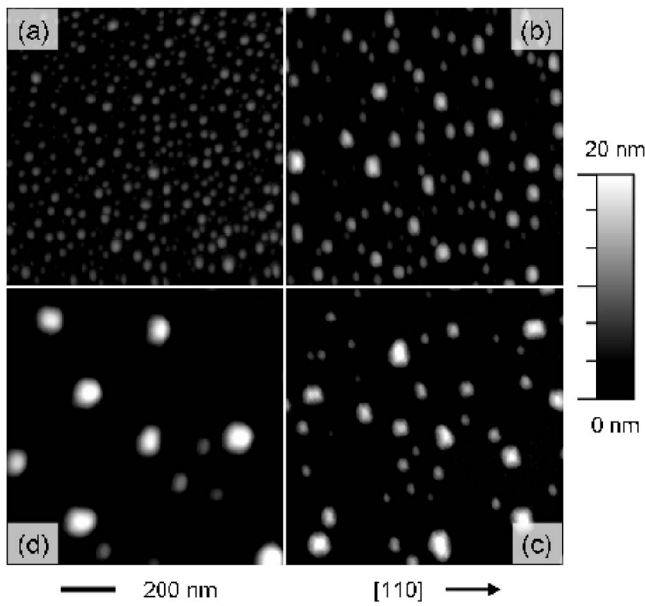


FIG. 1. AFM images of C-induced Ge QDs grown on strained $\text{Si}_{1-x}\text{Ge}_x$ buffer layers with (a) 8%, (b) 20%, (c) 44%, and (d) 64% Ge contents.

1(b)–1(d)] with the consequent increase in average island size.

Samples have been characterized *ex situ* by Raman spectroscopy to obtain information on strain and composition of the nanostructures. Three representative spectra are shown in Fig. 2. The composition of the SiGe alloy constituting the buffer layer can be determined from the position of the Si–Ge phonon mode apparent in the 400 cm^{-1} spectral range, considering that the built-in strain of the buffer layer is given by its pseudomorphic growth on the Si substrate. For the highest Ge content of the buffer layer (see bottom spectrum in Fig. 2) we can also resolve at least one of the local Si–Si modes of the SiGe alloy. Its position confirms the values of composition and strain from the Si–Ge mode. The peak at

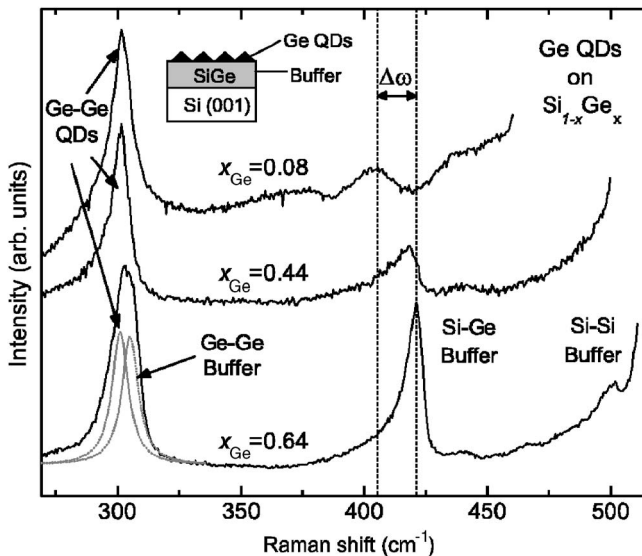


FIG. 2. Raman spectra of QD ensembles grown on $\text{Si}_{1-x}\text{Ge}_x$ buffer layers with contents of $x = 0.08$, 0.44 , and 0.64 . The assignment of the various Raman peaks to the different local Ge–Ge, Si–Ge, and Si–Si modes of the buffer layer and the dots is indicated. The dashed vertical lines put in evidence the frequency shift of the Si–Ge mode. The inset shows a sketch of a sample with uncapped Ge dots.

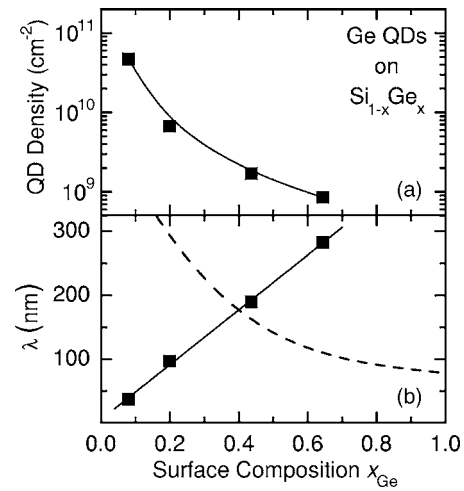


FIG. 3. Solid symbols correspond to (a) the island density and (b) the average interdot spacing vs the Ge content of the buffer layer, as obtained from optical spectroscopy. Solid lines are guides to the eyes. Dashed curve in (b) represents the roughness wavelength for SiGe films on Si calculated in Ref. 17 to explain the experimental data of Refs. 5 and 6.

301.3 cm^{-1} is ascribed to the Ge–Ge phonon mode of the Ge QDs and its spectral position is indicative of a very high Ge content of $x > 0.90$ and almost complete strain relaxation ($\epsilon_{\parallel} \approx -0.005$).¹⁵ We point out that for the buffer layer with highest Ge concentration we expected its Ge–Ge mode to be observable in Raman spectra as well at $\sim 305\text{ cm}^{-1}$. In fact, its contribution to the Ge–Ge phonon peak of the dots can be spectrally deconvoluted by fitting this peak with two Lorentzians, as illustrated by the dotted curves in Fig. 2.

The C-induced positioning of the preferential nucleation sites for the Ge dots is leading to the final topography observed for the different samples of Fig. 1. Such changes in topography are clearly related to the interplay between pre-deposited carbon and the Ge composition of the buffer layer constituting the surface where Ge adatoms move during growth but before being incorporated into a QD. In Fig. 3 we plot the dot density and average interdot spacing λ versus the Ge composition of the buffer layer, represented by the solid symbols. The striking result of this work concerns the observed tendency of the dot density which exhibits a significant, monotonous decrease by two orders of magnitude with increasing Ge content in the buffer layer from 0% up to $\sim 60\%$ whereas the interdot separation represented by λ increases.

According to thermodynamic models, strained SiGe layers are susceptible to evolve into morphological instabilities (ripples) which can form a cell pattern with a characteristic roughness wavelength λ .^{5,6} Although such low aspect ratio mounds are still highly strained, the slight relaxation occurring at their apex is enough to act as a template for preferential nucleation of bigger, further relaxed islands during the subsequent Ge deposition. In this picture the resulting average dot spacing matches the roughness wavelength λ . This model¹⁷ which describes well the experimental results of Refs. 5 and 6 predicts λ to scale as x_{Ge}^{-1} (see dashed curve in Fig. 3). This result is totally at odds with our observation of an almost linear increase of λ with Ge content when carbon has been predeposited onto the SiGe buffer layer.

If, in contrast, ripple formation was not responsible for preferential dot nucleation, one should assume that QDs nucleate at random sites and that the interdot spacing is de-

terminated by the adatom diffusion length in a kinetically limited growth regime.¹⁰ In this case, the dot density depends primarily on the surface Ge adatom mobility which, in turn, is related to the average roughness (but not in the form of ripples!) of the SiGe layer. The latter is known to increase with increasing Ge concentration,¹⁸ implying an increment of dot density in the $(1-3) \times 10^9 \text{ cm}^{-2}$ range as was previously reported.¹⁹ Obviously, this model also fails to pinpoint the growth mechanism at work in our case since results in Fig. 3 show the opposite trend in a much wider range of achievable dot densities ($10^9-10^{11} \text{ cm}^{-2}$).

In order to explain our experimental findings we need to take into account the effects of the submonolayer of carbon. Impurity atoms are known to cause enhanced surface roughness,²⁰ thus resulting in an increased dot density but this alone does not explain straightforwardly the observed dependence on Ge composition of the buffer layer. We propose a mechanism by which the chemical interactions among Si, Ge, and C drive the growth process. The Si-C attractive interaction favors C condensation, leading to the appearance of $c(4 \times 4)$ reconstruction patches¹⁴ also associated with an enhanced surface roughness. If the carbon is deposited on a layer containing Ge, the Ge-C repulsion²¹ induces phase separation and depending on Ge content the C-induced reconstruction patches become increasingly fragmented, being the C atoms progressively incorporated at random sites in the film.²² The key point is that the formation of the reconstruction patches produces a significant quenching of the Ge adatom diffusion, which within the kinetic model implies the self-assembled growth of a high density of Ge dots. With increasing Ge content of the buffer layer the C-induced patches gradually disappear, the surface roughness diminishes, and the Ge adatom diffusivity becomes enhanced, resulting in lower dot densities. This scenario is consistent with our recent work addressing the influence of Si interdiffusion when the carbon-induced QDs are grown on pure Ge wetting layers deposited at different temperatures.¹⁵ Again the dot density increases with increasing deposition temperature of the wetting layer, i.e., with higher Si content of the surface onto which the dots nucleate.

In conclusion, we have shown that the self-organized growth of Ge islands is fundamentally affected by the predeposition of a carbon submonolayer on a strained SiGe buffer layer. The relevant parameter which allows for a control of dot topography is the Ge content of the SiGe alloy. The result is a monomodal distribution of Ge rich quantum dots with an areal density which can be adjusted over a wide range ($10^9-10^{11} \text{ cm}^{-2}$) just by changing the Ge composition of the

SiGe buffer/wetting layer. The results are explained using a kinetically limited model for the growth mechanism which accounts for the interplay of chemical interactions among C, Si, and Ge as the determinant factor influencing Ge adatom mobility. This provides us with a powerful growth protocol for better design of Ge quantum dot nanostructures for device applications.

The authors are grateful to the Spanish Ministerio de Educación y Ciencia for support through MAT2003-00738. One of the authors (A.B.) also acknowledges an FPI fellowship. Another author (A.R.G.) is an ICREA Research Professor.

- ¹G. Capellini, M. D. Seta, F. Evangelisti, V. A. Zinovyev, G. Vastola, F. Montalenti, and L. Miglio, *Phys. Rev. Lett.* **96**, 106102 (2006).
- ²F. Ratto, A. Locatelli, S. Fontana, S. Kharrazi, S. Ashtaputre, S. K. Kulkarni, S. Heun, and F. Rosei, *Phys. Rev. Lett.* **96**, 096103 (2006).
- ³J. M. Baribeau, X. Wu, N. L. Rowell, and D. J. Lockwood, *J. Phys.: Condens. Matter* **18**, R139 (2006).
- ⁴A. Karmous, A. Cuenat, A. Ronda, I. Berbezier, S. Atha, and R. Hull, *Appl. Phys. Lett.* **85**, 6401 (2004).
- ⁵P. Sutter and M. G. Lagally, *Phys. Rev. Lett.* **84**, 4637 (2000).
- ⁶R. M. Tromp, F. M. Ross, and M. C. Reuter, *Phys. Rev. Lett.* **84**, 4641 (2000).
- ⁷I. Berbezier, M. Abdallah, A. Ronda, and G. Bremond, *Mater. Sci. Eng., B* **69-70**, 367 (2000).
- ⁸B. Ismail, M. Descoins, A. Ronda, F. Bassani, G. Bremond, H. Maaref, and I. Berbezier, *J. Vac. Sci. Technol. B* **23**, 242 (2005).
- ⁹I. Berbezier, A. Ronda, A. Portavoce, and N. Motta, *Appl. Phys. Lett.* **83**, 4833 (2003).
- ¹⁰H. J. Kim, Z. M. Zhao, and Y. H. Xie, *Phys. Rev. B* **68**, 205312 (2003).
- ¹¹M. Shaleev, A. Novikov, O. Kuznetsov, A. Yablonsky, N. Vostokov, Y. Drozdov, D. Lobanov, and Z. Krasilnik, *Mater. Sci. Eng., B* **124-125**, 466 (2005).
- ¹²H. Kim, C. Shin, and J. Chang, *Appl. Surf. Sci.* **252**, 1476 (2005).
- ¹³O. G. Schmidt, C. Lange, K. Eberl, O. Kienzle, and F. Ernst, *Appl. Phys. Lett.* **71**, 2340 (1997).
- ¹⁴O. Leifeld, A. Beyer, D. Grutzmacher, and K. Kern, *Phys. Rev. B* **66**, 125312 (2002).
- ¹⁵A. Bernardi, J. O. Ossó, M. I. Alonso, A. R. Goñi, and M. Garriga, *Nanotechnology* **17**, 2602 (2006).
- ¹⁶D. Perovic', B. Bahierathan, H. Lafontaine, D. Houghton, and D. McComb, *Physica A* **239**, 11 (1997).
- ¹⁷B. J. Spencer, P. W. Voorhees, and J. Tersoff, *Phys. Rev. B* **64**, 235318 (2001).
- ¹⁸G. G. Jernigan and P. E. Thompson, *Surf. Sci.* **516**, 207 (2002).
- ¹⁹D. Lobanov, A. Novikov, N. Vostokov, Y. Drozdov, A. Yablonskiy, Z. Krasilnik, M. Stoffel, U. Denker, and O. Schmidt, *Opt. Mater. (Amsterdam, Neth.)* **27**, 818 (2005).
- ²⁰G. G. Jernigan and P. E. Thompson, *Thin Solid Films* **472**, 16 (2005).
- ²¹P. C. Kelires, *Phys. Rev. Lett.* **75**, 1114 (1995).
- ²²A. Sakai, Y. Torige, M. Okada, H. Ikeda, Y. Yasuda, and S. Zaima, *Appl. Phys. Lett.* **79**, 3242 (2001).